



Post-CHF heat transfer during two-phase upflow boiling of R-407C in a vertical pipe

R. Sindhuja^a, A.R. Balakrishnan^{a,*}, S. Srinivasa Murthy^b

^a Department of Chemical Engineering, Indian Institute of Technology Madras, Chennai 600 036, India

^b Department of Mechanical Engineering, Indian Institute of Technology Madras, Chennai 600 036, India

ARTICLE INFO

Article history:

Received 26 January 2008

Accepted 30 July 2009

Available online 6 September 2009

Keywords:

Boiling heat transfer

Post critical heat flux

Vertical pipe

R-407C

ABSTRACT

This paper reports a study of heat transfer in the post-critical heat flux (post-CHF) regime under forced convective upflow conditions in a uniformly heated vertical tube of 12.7 mm internal diameter and 3 m length. Experiments were conducted with non-azeotropic ternary refrigerant mixture R-407C for reduced pressures ranging from 0.37 to 0.75, mass flux values from 1200 to 2000 kg/m² s and heat flux from 50 to 80 kW/m². Data shows a considerable effect of system pressure on the post-CHF heat transfer coefficient for specified mass and heat fluxes. The post-CHF heat transfer coefficients for R-407C are compared with three existing correlations which are found to over predict the current data. A modified correlation to represent the experimental data for R-407C is presented.

© 2009 Elsevier Ltd. All rights reserved.

1. Introduction

Convective boiling at high heat flux levels above the critical heat flux (CHF) is known as post-CHF heat transfer and is of importance in steam generators, nuclear reactors, cryogenic systems, refrigeration plants, etc. At the dryout (DO) location, the liquid film disappears resulting in the deterioration of convective heat transfer mechanism due to poor heat transfer characteristics of the vapor. Various physical mechanisms governing post-dryout heat transfer have been reviewed in the literature [1]. Post-dryout heat transfer studies using thermal non-equilibrium methods available for the prediction of post-dryout surface temperature [2,3] and analytical models for the dispersed flow regime have also been reported [4,5].

Ünal and Van Gasselt [6] conducted experiments on post-dryout heat transfer in a non-uniformly heated steam generator tube of 10 m length and 7.86 mm ID and for a pressure range of 14.8–19.9 MN/m². Based on this experimental data and existing literature data on uniformly heated tubes, a correlation for the estimation of post-dryout heat transfer coefficient was developed using dimensional analysis. This correlation is applicable for both uniform and non-uniform heated tubes. Nishikawa et al. [7] experimentally studied the post-dryout heat transfer at subcritical pressures with Refrigerant 22 in an upward flowing circular tube. A new correlation was proposed by introducing a non-dimensional parameter to take into account the non-equilibrium existing between the vapor and liquid droplets. This correlation was therefore able to successfully predict the wall temperatures at subcritical pressures, whereas

conventional models failed to reproduce the experimental measurements. Experimental studies on flow visualization have also been reported in steady state inverted annular flow film boiling of Refrigerant 113 in a transparent test section to investigate the effects of jet core hydrodynamics and correlate the axial extent of each of the flow zone [8,9]. Kefer et al. [10] performed experimental investigations of post-dryout heat transfer on horizontal tubes and inclined tubes to quantify the effects of gravity on flow patterns and heat transfer. Effect of curvature on post-dryout dispersed flow in complex geometries like coils and bends have been studied by Wang and Mayingier [11].

Attempts have also been made to predict dryout and post-dryout heat transfer by incorporating the phenomenological models in a three-fluid model framework in which the mass, momentum and energy conservation equations are solved simultaneously for three phases namely, the liquid film, the liquid droplets and the vapor. Hoyer [12] proposed a set of constitutive relations to supplement the conservation equations and used the data of Becker et al. [13,14] to validate the model up to 70 bar with uniform and non-uniform axial heat flux distribution. Hoyer also compared the wall temperature variation in the post-dryout region for selected cases and reported good agreement. Recently, Jayanti and Valette [15] presented a one-dimensional three-fluid model for the prediction of dryout and post-dryout heat transfer at high pressures ($P/P_{cr} > 0.3$). They reported good agreement with the data of Becker et al. [13] for the dryout quality and the tube wall temperature variation in the post-dryout region except for the cases of low mass flux at high pressures.

As a logical sequel to the development of the successful CHF look-up table by Groeneveld et al. [16], an improved look-up table for film boiling heat transfer coefficients was derived for

* Corresponding author. Tel.: +91 4422574680; fax: +91 4422574652.
E-mail address: arbala@iitm.ac.in (A.R. Balakrishnan).

Nomenclature

| | |
|-------|--------------------------------------|
| D | diameter, m |
| g | acceleration due to gravity, m/s^2 |
| G | mass flux, $kg/m^2 s$ |
| h | heat transfer coefficient, $W/m^2 K$ |
| H | enthalpy, kJ/kg |
| k | thermal conductivity, W/mK |
| L | length of the tube, m |
| m | mass flow rate, m/s |
| P | pressure, bar |
| P_R | reduced pressure = P/P_c |
| q | heat flux, kW/m^2 |
| T | temperature, $^{\circ}C$ |
| x | quality |
| z | location, m |

Dimensionless numbers

| | |
|----|--------------------------------|
| Nu | Nusselt number = hD/k |
| Pr | Prandtl number = $C_p\mu/k$ |
| Re | Reynolds number = $Dv\rho/\mu$ |

Greek symbols

| | |
|--------|------------------------|
| ρ | density, kg/m^3 |
| μ | viscosity, $N s/m^2$ |
| Φ | surface tension, N/m |

Subscripts

| | |
|------|-------------------------|
| cr | critical |
| CHF | critical heat flux |
| b | bulk fluid |
| Exp | experimental |
| f | film |
| i | inner |
| l | liquid |
| PCHF | post-critical heat flux |
| Pre | predicted |
| s | saturation |
| sub | subcooling |
| v | vapor |
| w | wall |

steam-water flow inside vertical tubes [17]. Significant improvements were made to the Lueng et al. [18,19] look-up table referred to as PDO-LW-96 in order to expand the database of the original table, thus providing a better accuracy for calculating film boiling heat transfer coefficients. Recently, Vijayarangan [20] conducted experimental studies to obtain post-CHF data for R-134a over a wide range of pressures approaching critical conditions. It was found that the correlations of Groeneveld [21] and Ünal and Van Gasselt [6] failed to predict the post-dryout heat transfer coefficient at high reduced pressures approaching critical conditions and therefore a new correlation was developed by modifying the Groeneveld [21] correlation by correcting for the over prediction of post-dryout heat transfer coefficients at high reduced pressures.

The experimental studies reported on CHF and post-CHF behavior are limited to steam-water and pure refrigerants. Even though

several non-azeotropic refrigerant mixtures of hydrofluorocarbons (HFCs) have been accepted as replacements for the chlorofluorocarbon (CFC) refrigerants, the post-CHF behavior of such mixtures has not been addressed. It was earlier observed that DO and the corresponding CHF are mainly a result of hydrodynamic behavior and mixture effects are relatively negligible [22,23]. In the present work, an attempt is made to obtain the post-CHF data for ternary refrigerant mixture R-407C considering it to be an equivalent pure fluid with an overall bulk fluid composition. It is to be noted that CHF in the present study is concerned with the high quality DO corresponding to annular flow regime. The data for R-407C is obtained under vertical upflow conditions over a range of system pressure, mass flux and heat flux conditions with a fixed inlet subcooling conditions. In large evaporators with multiple-parallel refrigerant flow paths, a significant evaporation area is present in

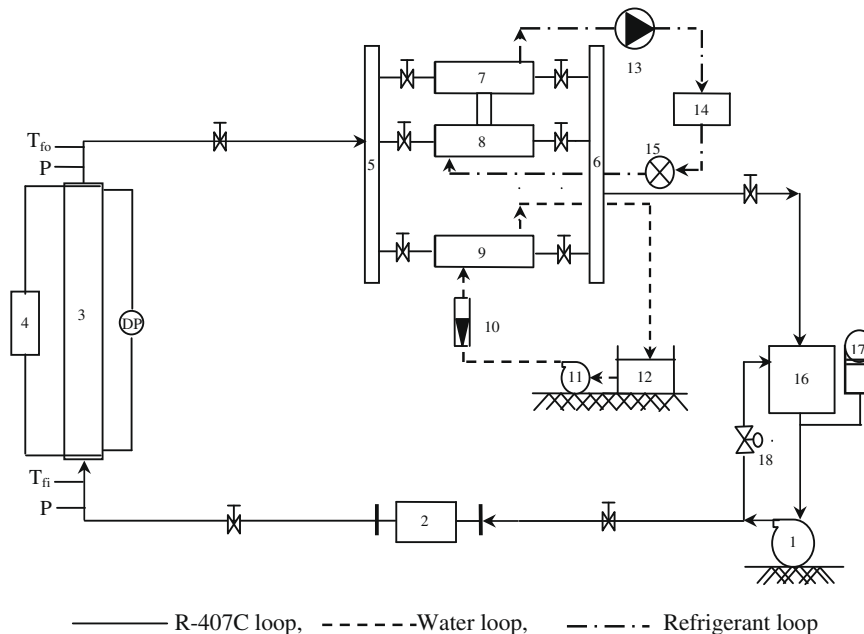


Fig. 1. Schematic diagram of the experimental set-up. (1) Refrigerant circulating pump; (2) mass flow meter; (3) test section; (4) DC rectifier; (5) inlet header; (6) outlet header; (7) low temperature condenser; (8) medium temperature condenser; (9) water cooled condenser; (10) rotameter; (11) water circulating pump; (12) thermostatic container; (13) compressor; (14) condenser of refrigeration system; (15) expansion valve; (16) R-407C receiver tank; (17) piston type accumulator; (18) by-pass valve; P – pressure indicator; DP – differential pressure indicator; T_{in} – inlet temperature indicator; T_{out} – outlet temperature indicator.

the form of vertical headers or distributors. Moreover, some special evaporator designs (e.g. flooded evaporators) invariably contain vertical tubes. Hence, a knowledge of boiling of refrigerants in vertical tubes is essential.

2. Experimental procedure

The experimental set-up used in the present investigation consists of the primary loop (or the working fluid loop), the chilling unit loop, the cooling water loop and the data acquisition system. The schematic diagram of the experimental set-up is shown in Fig. 1 and the details of the instrumentation on the test section are shown in Fig. 2. The set-up has been explained in detail earlier [23].

The post-CHF experiments were conducted as follows. R-407C from the storage tank is first circulated under subcooled liquid conditions through the test section and the rest of the loop with the help of the canned motor pump. The valves connecting the pressure tapping lines to the test section are opened so that any vapor present is removed. Heat is applied to the test section and the pressure is set to the desired value. The pressure in the test loop is adjusted by the piston accumulator. Once the system is stabilized at predetermined values of inlet temperature, mass flux, heat flux and pressure, the data from the pressure transducer, differential pressure transducer, tube wall temperatures along with the fluid inlet and outlet temperatures and mass flow rates are recorded through the data acquisition system. The experiments are repeated for different flow rates and pressures. The temperature of the fluid

Table 1

Range of parameters investigated in the present study.

| | |
|---------------------------|--|
| P (bar) | 17, 20, 22.5, 25, 27.5, 30, 32.5, 35 |
| P_R | 0.37, 0.43, 0.48, 0.54, 0.59, 0.64, 0.70, 0.75 |
| G (kg/m ² s) | 1200, 1400, 1600, 1800, 2000 |
| q (kW/m ²) | 50, 60, 70, 80 |
| T_{sub} (°C) | 3 |

at the inlet of the test section is maintained by controlling the temperature and the mass flow rate of cooling water flowing through the heat exchanger. The post-CHF experiments were conducted in the pressure range of 17–35 bar (corresponding reduced pressure range is 0.37–0.75), over a mass flux range of 1200–2000 kg/m² s and at four heat fluxes values of 50, 60, 70 and 80 kW/m². The inlet subcooling was maintained at 3 °C for all cases. Typically, CHF rarely occurred under the lowest heat flux, whereas under the higher heat flux values, existence of CHF was observed. The CHF analysis has been reported in detail earlier [23].

The post-CHF heat transfer coefficient at any axial location is determined from the measured wall temperature and the estimated bulk fluid temperature beyond the dryout point at that location. The post-CHF heat transfer coefficient is defined by the following equation:

$$h_{pCHF} = \frac{q}{(T_{w,i} - T_s)} \tag{1}$$

where q represents the applied heat flux and $T_{w,i}$ the inner wall temperature calculated from the measured outer wall temperature using one-dimensional radial heat conduction equation. T_s is the saturation temperature for pure fluids.

For binary or multicomponent mixtures, T_s is replaced by the local bubble point temperature or the bulk fluid temperature (T_b) corresponding to the local bulk liquid composition and the local saturation pressure and is calculated using the Refprop (version 7) simulation tool [24]. The calculation procedure has been explained in detail in the previous work [23]. The thermophysical properties of R-407C are given in Table 2.

3. Results and discussion

Post-CHF experiments have been carried out over a range of test section pressures and mass fluxes at fixed inlet subcooling of 3 °C. The overall test matrix is summarized in Table 1 in terms of the range of parameters investigated.

The typical variation of the wall temperature for different pressures at a constant mass flux of 200 kg/m² s has been discussed in the earlier work [23]. It is to be noted that at the dryout point, the wall temperature rises suddenly due to the deterioration of the convective heat transfer mechanism. The sudden rise in wall temperature at the CHF is a strong function of the system pressure. The wall temperature varies from 100 °C at a reduced pressure of 0.32 to about 20 °C at a reduced pressure of 0.90.

A total of 825 post-CHF wall temperature data points have been collected with a dryout quality greater than 0.2 and wall superheat greater than 10 °C in the post-CHF regime. The variation of the wall superheat defined as ($T_w - T_b$) for these temperatures is plotted as a function of reduced pressure in Fig. 3. As mentioned earlier, the wall superheat decreases significantly for higher values of reduced pressures.

The experimentally determined heat transfer coefficient is plotted in Fig. 4. It can be seen that heat transfer coefficient values increase correspondingly at higher reduced pressures. These results are in general agreement with the trends observed for the single-component (R-134a) refrigerant system [20].

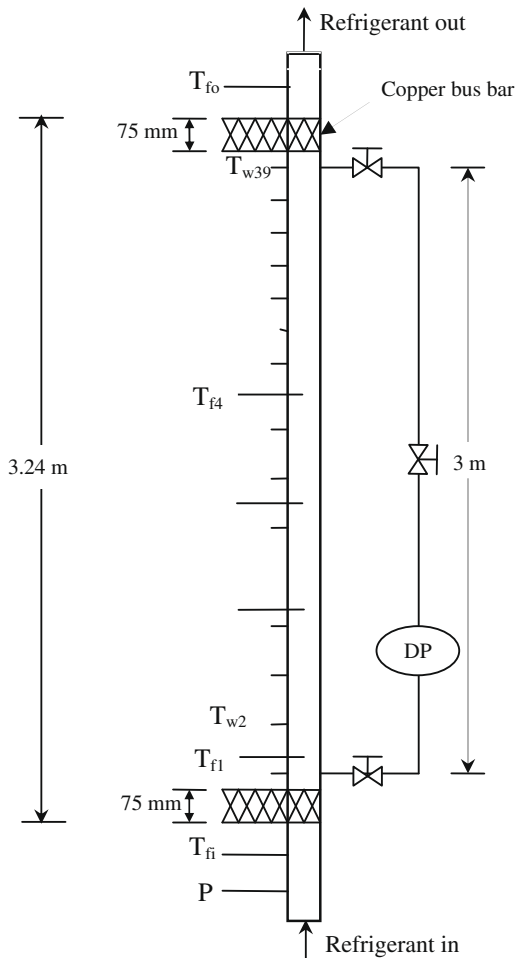


Fig. 2. Schematic diagram of vertical upflow test section.

Table 2
Thermal properties of R-407C [24].

| P, MPa | Liq T, °C | Vap T, °C | Liq ρ, kg/m ³ | Vap ρ, kg/m ³ | Liq H, kJ/kg | Vap H, kJ/kg | Liq Cp, kJ/kg K | Vap Cp, kJ/kg K | Liq k, mW/mK | Vap k, mW/mK | Liq μ, μPa s | Vap μ, μPa s | Liq σ, N/m | Vap σ, N/m |
|--------|-----------|-----------|--------------------------|--------------------------|--------------|--------------|-----------------|-----------------|--------------|--------------|--------------|--------------|------------|------------|
| 0.1 | -43.9 | -36.9 | 1381.5 | 4.5735 | 140.31 | 389.59 | 1.3121 | 0.78553 | 124.65 | 9.2773 | 404.47 | 10.063 | 0.01787 | 0.01696 |
| 0.2 | -28.41 | -21.69 | 1333 | 8.8131 | 160.87 | 398.23 | 1.3394 | 0.8476 | 115.84 | 10.315 | 316.54 | 10.757 | 0.01525 | 0.01449 |
| 0.3 | -18.19 | -11.66 | 1299.5 | 12.989 | 174.71 | 403.62 | 1.3624 | 0.89451 | 110.17 | 11.029 | 272.44 | 11.22 | 0.01356 | 0.01289 |
| 0.4 | -10.33 | -3.971 | 1272.8 | 17.154 | 185.52 | 407.55 | 1.3834 | 0.93446 | 105.89 | 11.615 | 243.98 | 11.576 | 0.01229 | 0.01168 |
| 0.5 | -3.854 | 2.3605 | 1250.1 | 21.334 | 194.56 | 410.64 | 1.4032 | 0.97045 | 102.41 | 12.129 | 223.34 | 11.866 | 0.01127 | 0.01071 |
| 0.6 | 1.7039 | 7.7871 | 1230 | 25.545 | 202.42 | 413.15 | 1.4224 | 1.004 | 99.466 | 12.594 | 207.33 | 12.109 | 0.01040 | 0.00988 |
| 0.7 | 6.6013 | 12.563 | 1211.7 | 29.796 | 209.44 | 415.25 | 1.4413 | 1.036 | 96.895 | 13.026 | 194.35 | 12.318 | 0.00965 | 0.00916 |
| 0.8 | 10.999 | 16.845 | 1194.9 | 34.098 | 215.83 | 417.03 | 1.46 | 1.067 | 94.607 | 13.436 | 183.47 | 12.499 | 0.00899 | 0.00853 |
| 0.9 | 15.002 | 20.739 | 1179.1 | 38.456 | 221.71 | 418.57 | 1.4789 | 1.0976 | 92.539 | 13.851 | 174.15 | 12.657 | 0.00839 | 0.00796 |
| 1 | 18.686 | 24.317 | 1164.1 | 42.877 | 227.19 | 419.89 | 1.4979 | 1.1282 | 90.649 | 14.257 | 166 | 12.795 | 0.00785 | 0.00744 |
| 1.1 | 22.105 | 27.633 | 1149.9 | 47.367 | 232.34 | 421.03 | 1.5172 | 1.1589 | 88.904 | 14.659 | 158.78 | 12.915 | 0.00735 | 0.00697 |
| 1.2 | 25.301 | 30.728 | 1136.2 | 51.932 | 237.2 | 422.03 | 1.537 | 1.1902 | 87.282 | 15.045 | 152.3 | 13.128 | 0.00690 | 0.00653 |
| 1.3 | 28.304 | 33.632 | 1123 | 56.576 | 241.82 | 422.89 | 1.5572 | 1.2221 | 85.763 | 15.442 | 146.43 | 13.325 | 0.00647 | 0.00612 |
| 1.4 | 31.141 | 36.372 | 1110.2 | 61.306 | 246.24 | 423.63 | 1.578 | 1.2549 | 84.333 | 15.842 | 141.05 | 13.521 | 0.00608 | 0.00574 |
| 1.5 | 33.832 | 38.966 | 1097.7 | 66.128 | 250.48 | 424.27 | 1.5996 | 1.2889 | 82.981 | 16.248 | 136.11 | 13.716 | 0.00571 | 0.00539 |
| 1.6 | 36.394 | 41.432 | 1085.5 | 71.047 | 254.57 | 424.8 | 1.6219 | 1.3242 | 81.698 | 16.66 | 131.52 | 13.911 | 0.00536 | 0.00506 |
| 1.7 | 38.839 | 43.783 | 1073.5 | 76.07 | 258.51 | 425.25 | 1.6452 | 1.361 | 80.475 | 17.081 | 127.24 | 14.107 | 0.00503 | 0.00474 |
| 1.8 | 41.181 | 46.029 | 1061.7 | 81.203 | 262.33 | 425.61 | 1.6695 | 1.3996 | 79.306 | 17.513 | 123.23 | 14.304 | 0.00472 | 0.00444 |
| 1.9 | 43.428 | 48.182 | 1050 | 86.454 | 266.05 | 425.89 | 1.695 | 1.4402 | 78.186 | 17.957 | 119.45 | 14.503 | 0.00442 | 0.00416 |
| 2 | 45.59 | 50.248 | 1038.5 | 91.831 | 269.66 | 426.1 | 1.7218 | 1.4831 | 77.11 | 18.416 | 115.88 | 14.704 | 0.00415 | 0.00390 |
| 2.1 | 47.673 | 52.236 | 1027.1 | 97.342 | 273.19 | 426.23 | 1.7502 | 1.5286 | 76.074 | 18.892 | 112.49 | 14.909 | 0.00388 | 0.00364 |
| 2.2 | 49.685 | 54.152 | 1015.7 | 103 | 276.64 | 426.29 | 1.7804 | 1.577 | 75.075 | 19.391 | 109.27 | 15.116 | 0.00363 | 0.00340 |
| 2.3 | 51.629 | 56 | 1004.4 | 108.8 | 280.02 | 426.28 | 1.8126 | 1.6288 | 74.109 | 19.912 | 106.18 | 15.329 | 0.00339 | 0.00317 |
| 2.4 | 53.513 | 57.786 | 993.12 | 114.78 | 283.34 | 426.2 | 1.847 | 1.6845 | 73.174 | 20.456 | 103.22 | 15.546 | 0.00316 | 0.00295 |
| 2.5 | 55.339 | 59.514 | 981.8 | 120.93 | 286.6 | 426.06 | 1.8842 | 1.7445 | 72.268 | 21.026 | 100.38 | 15.768 | 0.00293 | 0.00274 |
| 2.6 | 57.112 | 61.188 | 970.45 | 127.27 | 289.82 | 425.85 | 1.9244 | 1.8096 | 71.389 | 21.625 | 97.633 | 15.997 | 0.00272 | 0.00254 |
| 2.7 | 58.834 | 62.81 | 959.04 | 133.83 | 292.99 | 425.57 | 1.9681 | 1.8805 | 70.536 | 22.257 | 94.978 | 16.234 | 0.00252 | 0.00235 |
| 2.8 | 60.511 | 64.384 | 947.53 | 140.6 | 296.12 | 425.21 | 2.0161 | 1.9582 | 69.706 | 22.924 | 92.402 | 16.479 | 0.00233 | 0.00216 |
| 2.9 | 62.143 | 65.912 | 935.9 | 147.63 | 299.23 | 424.79 | 2.069 | 2.0439 | 68.899 | 23.631 | 89.895 | 16.734 | 0.00214 | 0.00199 |
| 3 | 63.734 | 67.397 | 924.11 | 154.93 | 302.31 | 424.29 | 2.1279 | 2.139 | 68.115 | 24.382 | 87.449 | 17 | 0.00197 | 0.00182 |
| 3.1 | 65.286 | 68.841 | 912.13 | 162.52 | 305.38 | 423.72 | 2.1938 | 2.2452 | 67.353 | 25.183 | 85.054 | 17.278 | 0.00180 | 0.00166 |
| 3.2 | 66.801 | 70.246 | 899.92 | 170.45 | 308.43 | 423.06 | 2.2682 | 2.3648 | 66.612 | 26.04 | 82.702 | 17.571 | 0.00163 | 0.00150 |
| 3.3 | 68.282 | 71.612 | 887.41 | 178.75 | 311.49 | 422.31 | 2.3531 | 2.5007 | 65.895 | 26.959 | 80.383 | 17.88 | 0.00148 | 0.00135 |
| 3.4 | 69.73 | 72.943 | 874.56 | 187.47 | 314.54 | 421.46 | 2.4511 | 2.6567 | 65.202 | 27.951 | 78.089 | 18.208 | 0.00133 | 0.00121 |
| 3.5 | 71.146 | 74.238 | 861.31 | 196.66 | 317.61 | 420.51 | 2.5655 | 2.8377 | 64.536 | 29.026 | 75.811 | 18.559 | 0.00119 | 0.00108 |
| 3.6 | 72.533 | 75.499 | 847.56 | 206.4 | 320.71 | 419.45 | 2.7011 | 3.0504 | 63.902 | 30.198 | 73.536 | 18.936 | 0.00105 | 0.00095 |
| 3.7 | 73.892 | 76.727 | 833.21 | 216.77 | 323.84 | 418.26 | 2.8645 | 3.3044 | 63.306 | 31.485 | 71.254 | 19.344 | 0.00092 | 0.00083 |
| 3.8 | 75.224 | 77.922 | 818.13 | 227.89 | 327.02 | 416.91 | 3.0653 | 3.6132 | 62.757 | 32.91 | 68.95 | 19.79 | 0.00079 | 0.00071 |
| 3.9 | 76.532 | 79.085 | 802.16 | 239.91 | 330.28 | 415.39 | 3.3183 | 3.9967 | 62.273 | 34.505 | 66.607 | 20.283 | 0.00068 | 0.00060 |
| 4 | 77.817 | 80.215 | 785.06 | 253.04 | 333.64 | 413.66 | 3.6469 | 4.4863 | 61.877 | 36.315 | 64.203 | 20.835 | 0.00056 | 0.00050 |
| 4.1 | 79.08 | 81.311 | 766.5 | 267.59 | 337.13 | 411.67 | 4.0915 | 5.1336 | 61.603 | 38.407 | 61.707 | 21.463 | 0.00046 | 0.00040 |
| 4.2 | 80.325 | 82.373 | 745.97 | 284.01 | 340.83 | 409.34 | 4.7261 | 6.0289 | 61.508 | 40.884 | 59.074 | 22.197 | 0.00036 | 0.00031 |
| 4.3 | 81.554 | 83.395 | 722.64 | 303.1 | 344.82 | 406.54 | 5.7054 | 7.35 | 61.68 | 43.928 | 56.23 | 23.082 | 0.00026 | 0.00022 |
| 4.5 | 83.997 | 85.287 | 658.77 | 357.31 | 354.74 | 398.22 | 11.047 | 13.563 | 62.675 | 53.531 | 47.945 | 25.818 | 0.00010 | 0.00007 |

3.1. Correlation of experimental data

Two well-established methods of predicting post-CHF heat transfer coefficient, namely, the correlation of Groeneveld [21] and the correlation of Ünal and Van Gasselt [6], as well as the Vijayarangan correlation [20] have been used for the prediction of the present data. The correlation of Groeneveld [21] is given below:

$$\text{Nu} = \frac{h_{\text{PCHF}} D}{k_v} = 1.09 \times 10^{-3} \left\{ \text{Re}_v \left[x + \frac{\rho_v}{\rho_l} (1-x) \right] \right\}^{0.989} \times \text{Pr}_v^{1.4} \left(1 - 0.1 \left(\frac{\rho_l}{\rho_v} - 1 \right)^{0.4} (1-x)^{0.4} \right)^{-1.15} \quad (2)$$

where Re_v and Pr_v are the Reynolds number and Prandtl number of the vapor phase.

Ünal and Van Gasselt [6], as mentioned earlier, analyzed a large body of data collected from both uniformly and non-uniformly heated vertical tubes and proposed the following correlation:

$$\text{Nu} = 0.0091 \left\{ \frac{GD}{\mu_f} \left[x + (1-x) \frac{\rho_v}{\rho_l} \right] \right\}^{1.154} \text{Pr}_f^{0.577} \left(\frac{k_f}{k_{cr}} \right)^{0.59} \left(\frac{T_f}{T_{cr}} \right)^{-2.17} \times \left[\text{Pr}_R^{0.212} (1 - \text{Pr}_R)^{-0.27} \right] \left[\frac{G^2}{\rho_l^2 Dg} \right]^{0.0396} \left[\frac{q}{H_1 G} \right]^{0.44} \quad (3)$$

where subscript f refers to the film temperature.

Vijayarangan [20] analyzed a large body of data for pure refrigerant R-134a covering wide range of pressures up to near critical conditions and correlated them as

$$\text{Nu} = \frac{h_{\text{PCHF}} D}{k_v} = 0.004 \left\{ \text{Re}_v \left[x + \frac{\rho_v}{\rho_l} (1-x) \right] \right\}^{0.9} \text{Pr}_v^{1.1} \text{Pr}_R^{-0.25} \quad (4)$$

The overall comparison of the above three correlations with the 825 data points for local heat transfer coefficients beyond CHF collected in the present study are shown in Figs. 5–7 respectively. It can be seen that Groeneveld [21] and Vijayarangan [20] correlations largely over predict the experimental data. Although Ünal and Van Gasselt [6] correlation agrees reasonably well with most of the data points lying within $\pm 30\%$ limits, there is a certain bias.

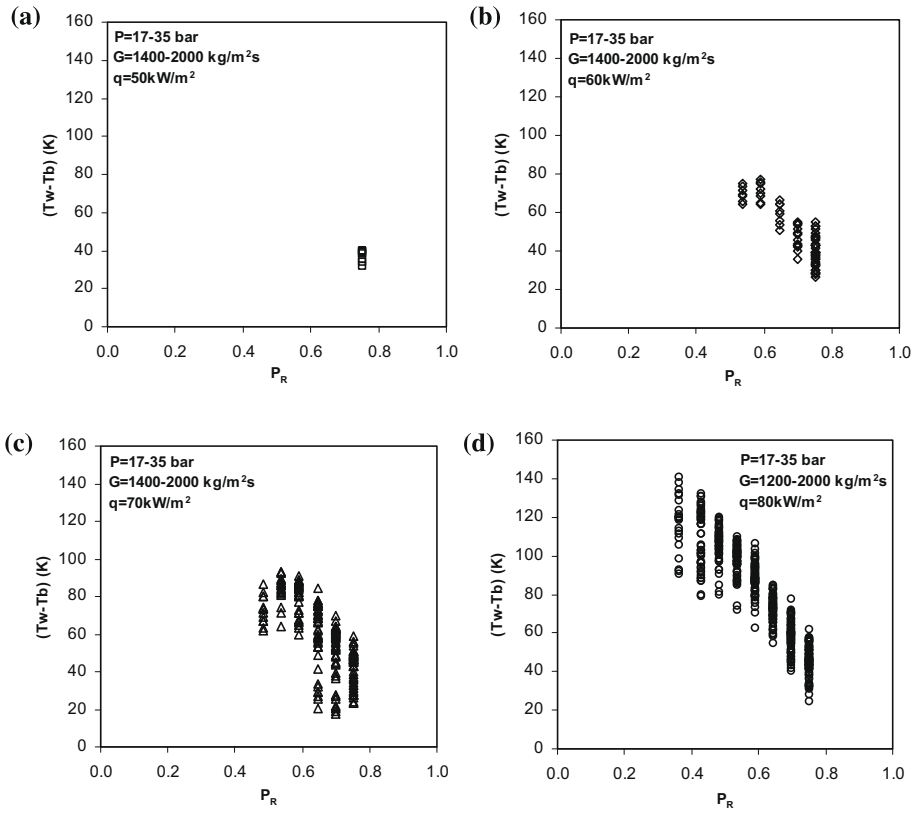


Fig. 3. Measured wall superheat as a function of reduced pressure for mass fluxes ranging from 1200 to 2000 kg/m² s and for heat fluxes of (a) 50, (b) 60, (c) 70 and (d) 80 kW/m².

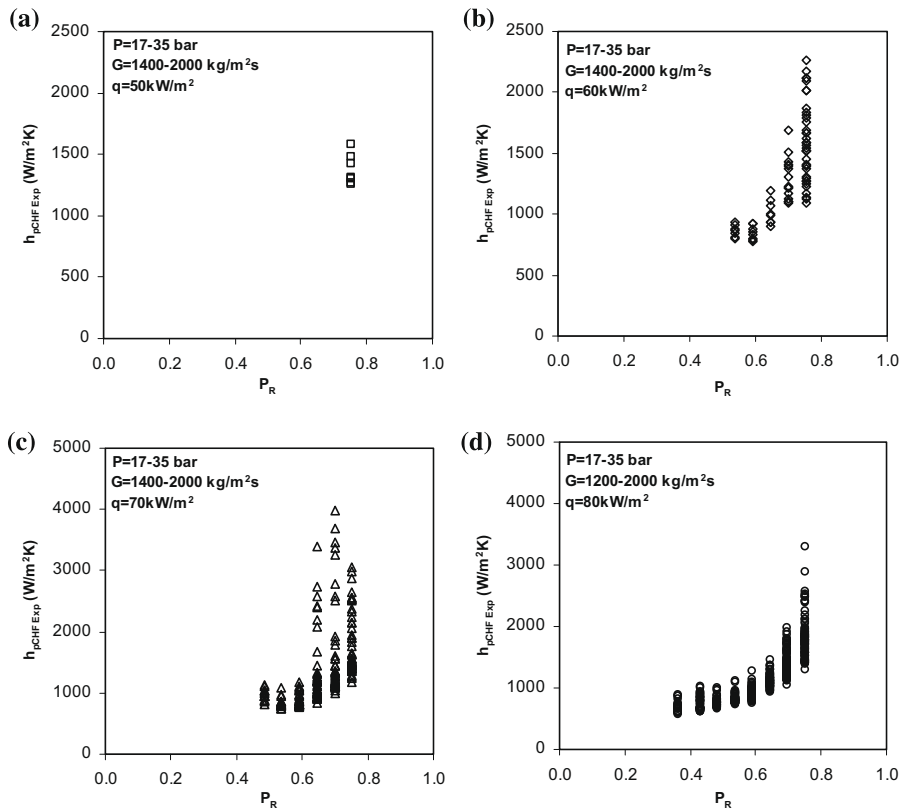


Fig. 4. Measured post-CHF heat transfer coefficient as a function of reduced pressure for mass fluxes ranging from 1200 to 2000 kg/m² s and for heat fluxes of (a) 50, (b) 60, (c) 70 and (d) 80 kW/m².

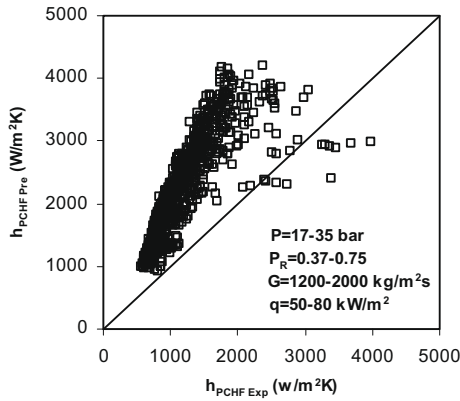


Fig. 5. Comparison of the present data on post-CHF heat transfer coefficient with Groeneveld [21] correlation.

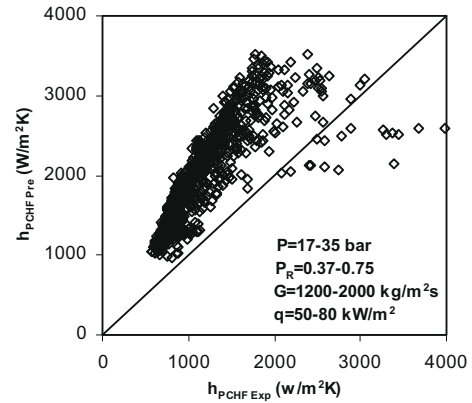


Fig. 7. Comparison of the present data on post-CHF heat transfer coefficient with Vijayarangan [20] correlation.

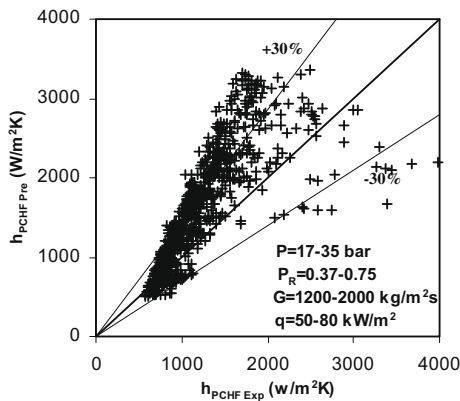


Fig. 6. Comparison of the present data on post-CHF heat transfer coefficient with Ünal and Van Gasselt [6].

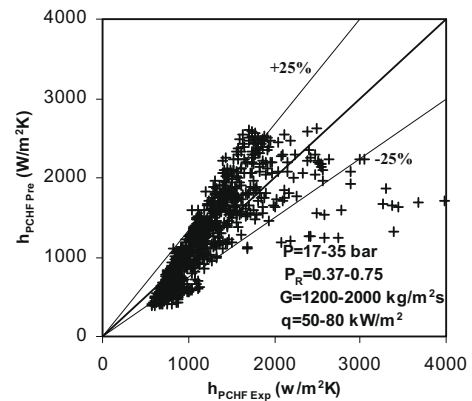


Fig. 8. Comparison of the present data on post-CHF heat transfer coefficient with the modified correlation.

One possible explanation for this bias is the fact that the Ünal and Van Gasselt [6] correlation was developed for a steam-water system and for high reduced pressures of 0.67–0.90.

In order to better fit the present data for ternary refrigerant mixtures, the slope of the Ünal and Van Gasselt [6] correlation has been modified. Fig. 8 shows the comparison of the present data with the modified correlation given below:

$$\text{Nu} = 0.0071 \left\{ \frac{GD}{\mu_f} \left[x + (1-x) \frac{\rho_v}{\rho_l} \right] \right\}^{1.154} \text{Pr}_f^{0.577} \left(\frac{k_f}{k_{cr}} \right)^{0.59} \left(\frac{T_f}{T_{cr}} \right)^{-2.17} \times \left[P_R^{0.212} (1 - P_R)^{-0.27} \right] \left[\frac{G^2}{\rho_l^2 D g} \right]^{0.0396} \left[\frac{q}{H_1 G} \right]^{0.44} \quad (5)$$

It is seen that the predicted post-CHF heat transfer coefficient values agree well with experimental data over the range of system pressures and that the bias seen in the original prediction of Ünal and Van Gasselt [6] correlation has been considerably reduced. The modified correlation predicts the present data for ternary refrigerants within the range of $\pm 25\%$. The range of the dimensionless groups for which the above correlation is valid is given by

$$P_R = 0.37-0.75$$

$$x = 0.22-0.73$$

$$\frac{\rho_v}{\rho_l} = 0.07-0.23$$

$$\text{Re}_v = 24 \times 10^4 - 60 \times 10^4$$

$$\text{Pr}_v = 1.15-1.81$$

3.2. Measurement uncertainties

Uncertainties in the experimental data were calculated using the error analysis suggested by Moffat [25]. In evaluation of the heat transfer coefficient, the inaccuracy is attributed to the errors in the heat flux and temperature measurements. In the present study the measured variables are the wall temperature, system pressure, differential pressure, mass flow rate, the voltage and current applied. The uncertainty in the measurement of temperature is $\pm 0.1\%$. The uncertainty in the measurement of mass flow rate is $\pm 0.5\%$. The uncertainty in the measurement of system pressure and differential pressure is $\pm 0.25\%$. There is a $\pm 1\%$ uncertainty in the measurement of both voltage and current which results in an uncertainty of $\pm 2.26\%$ in the heat flux for 50 kW/m^2 , $\pm 2.06\%$ for 60 kW/m^2 , $\pm 1.91\%$ for 70 kW/m^2 and $\pm 1.79\%$ for 80 kW/m^2 . From these uncertainties the most probable errors in the heat transfer coefficients under the present operating condition ranged between 2.03% and 8.15%.

4. Conclusions

Experiments to determine post-CHF heat transfer coefficient have been conducted in a uniformly heated vertical tube with the ternary non-azeotropic refrigerant mixture R-407C. The post-CHF heat transfer coefficient is found to increase with the increase in reduced pressure as in the case of pure fluids. Existing correlations for pure fluids over predict the post-CHF heat transfer

coefficient data by a large margin over the entire range of investigation when applied for non-azeotropic refrigerant mixtures. A new correlation has been proposed in this paper by modifying the Ünal and Van Gasselt [6] correlation.

References

- [1] D.C. Groeneveld, Post-dryout heat transfer: physical mechanisms and a survey of prediction methods, *Nucl. Eng. Des.* 32 (1975) 283–294.
- [2] D.C. Groeneveld, G.G.J. Delorme, Prediction of thermal non-equilibrium in the post-dryout regime, *Nucl. Eng. Des.* 36 (1976) 17–26.
- [3] R.A. Moose, E.N. Ganic, On the calculation of wall temperatures in the post-dryout heat transfer region, *Int. J. Multiphase Flow* 8 (5) (1982) 525–542.
- [4] Y. Koizumi, T. Ueda, H. Tanaka, Post-dryout heat transfer to R-113 upward flow in a vertical tube, *Int. J. Heat Mass Transfer* 22 (1979) 669–678.
- [5] P. Saha, A non-equilibrium heat transfer model for dispersed droplet post-dryout regime, *Int. J. Heat Mass Transfer* 23 (1980) 483–492.
- [6] H.C. Ünal, M.L.G. Van Gasselt, Post-dryout heat transfer in steam generator tubes at high pressures, *Int. J. Heat Mass Transfer* 26 (3) (1983) 459–464.
- [7] K. Nishikawa, S. Yoshida, H. Mori, H. Takamatsu, Post-dryout heat transfer to Freon in a vertical tube at high subcritical pressures, *Int. J. Heat Mass Transfer* 29 (8) (1986) 1245–1251.
- [8] M. Ishii, G de Jarlais, Flow visualization study of inverted annular flow of post-dryout heat transfer region, *Nucl. Eng. Des.* 99 (1987) 187–199.
- [9] N.T. Obot, M. Ishii, Two-phase flow regime transition criteria in post-dryout region based on flow visualization experiments, *Int. J. Heat Mass Transfer* 31 (12) (1988) 2559–2570.
- [10] V. Kefer, W. Kohler, W. Kastner, Critical heat flux (CHF) and post-CHF heat transfer in horizontal and inclined evaporator tubes, *Int. J. Multiphase Flow* 15 (3) (1989) 385–392.
- [11] M.J. Wang, F. Mayinger, Post-dryout dispersed flow in circular bends, *Int. J. Multiphase Flow* 21 (3) (1995) 437–454.
- [12] N. Hoyer, Calculation of dryout and post-dryout heat transfer for tube geometry, *Int. J. Multiphase Flow* 24 (1998) 319–334.
- [13] K.M. Becker, C.H. Ling, S. Hedberg, G. Strand, An experimental investigation of post dryout heat transfer, Department of Nuclear Reactor Engineering, Royal Institute of Technology Report KTH-NEL-33, Stockholm, Sweden, 1983.
- [14] K.M. Becker, P. Askelijung, S. Hedberg, B. Söderquist, U. Kahlbom, An experimental investigation of the influence of axial heat flux distributions on post dryout heat transfer for flow of water in vertical tubes, Department of Nuclear Reactor Engineering, Royal Institute of Technology Report KTH-NEL-54, Stockholm, Sweden, 1992.
- [15] S. Jayanti, M. Valette, Prediction of dryout and post-dryout heat transfer at high pressures using a one-dimensional three-fluid model, *Int. J. Heat Mass Transfer* 47 (2004) 4895–4910.
- [16] D.C. Groeneveld, L.K.H. Leung, P.L. Kirillov, V.P. Bobkov, I.P. Smogalov, V.N. Vinogradov, X.C. Huang, E. Royer, The 1995 look-up table for critical heat flux in tubes, *Nucl. Eng. Des.* 163 (1996) 1–23.
- [17] D.C. Groeneveld, L.K.H. Leung, A.Z. Vasic, Y.J. Guo, S.C. Chend, A look-up table for fully developed film-boiling heat transfer, *Nucl. Eng. Des.* 225 (2003) 83–97.
- [18] L.K.H. Leung, N. Hammouda, D.C. Groeneveld, Development of a look-up table for film boiling heat transfer covering wide range of flow conditions, in: Proceedings of the Fifth International Conference on Simulation Methods in Nuclear Eng., vol. II Montreal, Canada, 8–11 September, (1996).
- [19] L.K.H. Leung, N. Hammouda, D.C. Groeneveld, A look-up table for film boiling heat transfer coefficients in tubes with vertical upward flow, in: Proceedings of the Eighth International Topical Meeting on Nuclear Reactor Thermal-Hydraulics (NURETH-8), Kyoto, Japan, 30 September – 4 October, 1997.
- [20] B.R. Vijayarangan, Studies on pressure drop and boiling heat transfer in two-phase flow at near critical conditions, Ph.D. Dissertation, Indian Institute of Technology Madras, India, 2005.
- [21] D.C. Groeneveld, Post dryout heat transfer at reactor operating conditions, Natl. Topical Meeting. Water Reactor Safety, American Nuclear Society Conference. 730304 Report AECL-4513, Atomic Energy of Canada, 1973.
- [22] G.P. Celata, M. Cumo, T. Setaro, Critical heat flux in upflow convective boiling of refrigerant binary mixtures, *Int. J. Heat Mass Transfer* 37 (7) (1994) 1143–1153.
- [23] R. Sindhuja, A.R. Balakrishnan, S. Srinivasa Murthy, Critical heat flux of R-407C in upflow boiling in a vertical pipe, *Appl. Therm. Eng.* 28 (2008) 1058–1065.
- [24] REFPROP, Version 7.0, NIST Standard Reference Database 23, National Institute of Standards and Technology, Gaithersburg, Maryland, USA, 1996.
- [25] R.J. Moffat, Describing the uncertainties in experimental results, *Exp. Therm. Fluid Sci.* 1 (1988) 3–17.